Progress In Electromagnetics Research M, Vol. 125, 11-19, 2024

PIER M

(Received 10 January 2024, Accepted 28 February 2024, Scheduled 8 March 2024)

Customizable Substrate Integrated Waveguide Based Dual Pole Band Pass Filter for X Band Application

Ruchi Paliwal*, Shweta Srivastava, and Reema Budhiraja

Jaypee Institute of Information Technology, Noida, India

ABSTRACT: This manuscript introduces an innovative customizable dual pole bandpass filter using a substrate-integrated waveguide technology on a conventional Rogers RT/Duroid 5880 high-frequency laminate. This structure is bifurcated into two identical cavity resonators to get the band stop-band pass-band stop behavior. The structure comprises lumped capacitors to indicate each resonator's operating frequency. Additionally, altering the capacitors in the proposed design facilitates the generation of the tunable dual pole in passband frequency, adding to its versatility. Further, measured and simulated results indicate that the design attains large tuning bandwidth, excellent insertion loss (better than 0.4 dB) and return loss ($>$ 22 dB), high Q-factor (11.8 to 16.87) with fractional bandwidth of 4.8% to 8.9% throughout the tuning range, affirming its practicality and functionality in X-band. A total of 12.3% of tunability is achieved from the structure.

1. INTRODUCTION

Substrate Integrated Waveguides (SIWs) are becoming more and more common in microwave/millimeter-wave circuit design due to their reduced conductor losses and greater integration possibilities than existing choices of planner bandpass filters. They provide the ability to create waveguide circuits using a metallic via-slot array, which is perfect for high-performance, small devices [1]. The importance of SIW technology has been highlighted by recent advancements in the efficiency and miniaturization of wireless communication components, especially in the creation of small SIW bandpass filters [2–4]. Half-mode SIW (HMSIW) and Folded half-mode SIW (FHMSIW) designs have significantly reduced the physical footprint of various RF components while maintaining excellent performance. They are widely used in power dividers, filters, and antennas, utilizing complex techniques like quarter-mode, half-mode, and folding SIW cavities [5, 6–13]. Further, it is especially significant to trace the progress of fixed/tunable filters. Frequency-tunable SIW resonators have made it possible to create frequency-tunable SIW filters, which have produced multifunctional, bandpass, and band-stop filters that meet the changing needs of today's wireless systems [14]. This study seeks to investigate the state-of-the-art mechanically tunable SIW filters and circuits [15] to highlight their vital role in improving the performance and compactness of today's RF modules. Tunable SIW filters are important for dynamic spectrum management, because of the necessity for the operation of frequency-agile and adaptive RF transceiver modules [16]. They are employed in defense tracking, control of air traffic and marine vessel traffic, weather monitoring, and vehicle speed detection. Their significance in the current communication infrastructure is highlighted by their capacity to adjust and react in real-time to varying frequency requirements [17–19].

In addition, these filters' usefulness is further increased by a range of tuning mechanisms that satisfy specific requirements related to operating power, design frequency, manufacturing complexity, and overall cost. The tunability of the SIW filter may be continuous or discrete depending upon the application. It may be categorized as mechanical and electronic tuning. Metallic screws, flaps, posts, the insertion of a dielectric rod, etc. [20–22] can be used to tune the filter mechanically while PIN diodes, varactor diodes, MEMS switches, etc. [24–29] can be used for electronic tuning. For the design and implementation of electronically reconfigurable filters, sophisticated DC bias circuits are required, which increases their size, complexity, and power consumption. On the other hand, mechanical tuning has its limitations, such as the low reconfigurability of components like screws or rods [30], complex integration, and material-induced losses. Additionally, downsizing is a challenge, making mechanical tuning less feasible for RF components that require compactness. It is important to mention that when it comes to filters used in Customer Premises Equipment (CPE), active tuning elements like diodes are not always necessary. Instead, different capacitor values can be used to operate CPE filters at various fixed frequencies. This is particularly significant because the use of varactor diodes can increase the loss, cost, and complexity of the filter. To address this issue, a simple tuning mechanism is proposed using a passive component to provide the customized tuning to the SIW band-pass filter operating in the X-band. The proposed SIW structure incorporates a customizable feature by changing the surface mount technology capacitors, allowing the same fabricated structure to be used at fixed but different frequencies by integrating different value capacitors so that the same filter can be rearranged to different channel frequencies for various CPEs.

In the context of the current work, a customizable band-pass filter is presented that makes use of an electrically adjustable

* Corresponding author: Ruchi Paliwal (ruchipaliwal06@gmail.com).

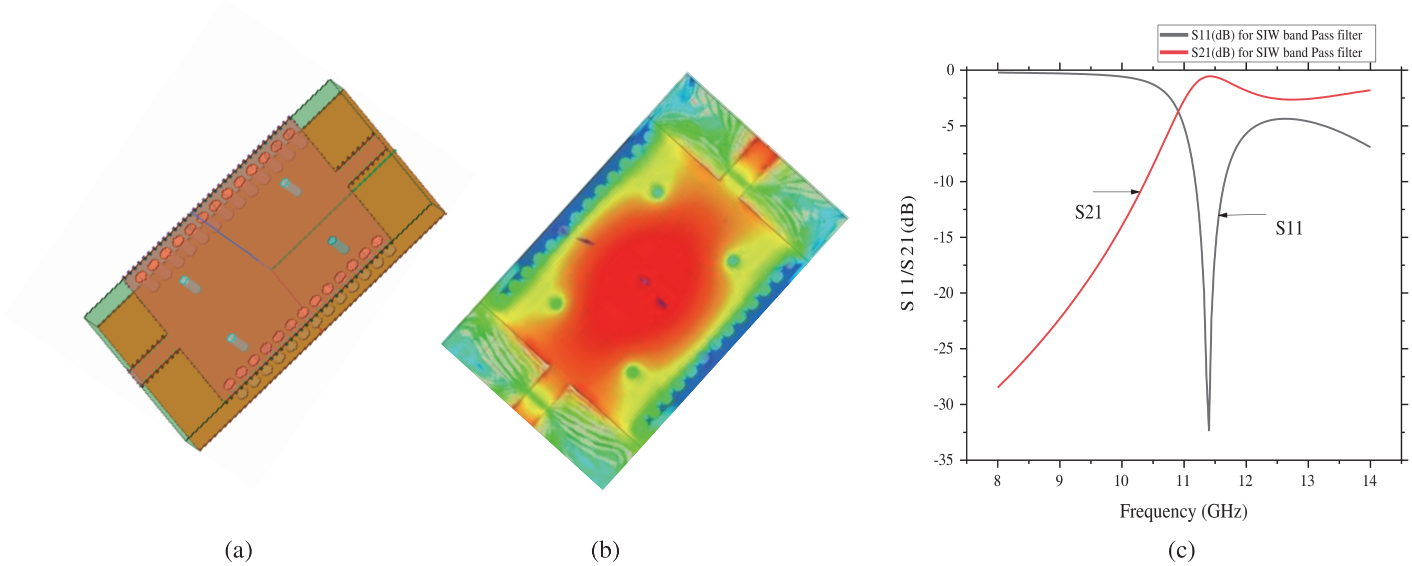

FIGURE 1. (a) Schematic of SIW band pass filter. (b) Electric Field distribution of SIW band pass filter. (c) Simulated S-parameters.

double pole SIW resonator, loaded with four capacitors on the top of the four perturbation vias. The center frequency of the filter can be adjusted from 10 to 12 GHz with the replacement of SMT capacitor values based on the user's demand. Insertion loss (better than 0.4 dB) is obtained in the operating frequency range with a fractional bandwidth (FBW) of 4.8% to 8.9%, and quality factor is in the range from 11.8 to 16.87. This research presents a complete study on the design and implementation of customizable BPF based on SIW, resulting in a cost-effective solution for advanced wireless systems.

The paper is structured as follows. Section 2 discusses the design and analysis of the proposed filter. It also discusses the tuning mechanism incorporated in the design. Section 3 discusses the experimental results and comparison with simulation results. Finally, a conclusion is made in Section 4.

2. PROPOSED TUNABLE FILTER

2.1. SIW Band Pass Filter Design

In Fig. 1(a), a schematic representation of a bandpass filter for X band is designed using the design equation which can be represented as:

$$W_{eff} = a - 1.08\frac{d^2}{p} + 0.1\frac{d^2}{a} \tag{1}$$

Where p = pitch (distance between consecutive vias), d = diameter of metal vias, and W_{eff} = effective width of SIW waveguide [31, 32]. To ensure effective design, the metal via's diameter needs to be

$$d < \frac{\lambda_g}{5} \tag{2}$$

where λg is the guided wavelength of a waveguide. The relation between the diameter of metal vias and the spacing between subsequent vias must be satisfied such that

$$P \leq 2d \tag{3}$$

Once the parameters are calculated, the inner side cavity is created with the help of the via post placed vertically in the SIW structure to get the bandpass response from the designed high pass filter as shown in Fig. 1(a). The simulated electric field distribution shown in Fig. 1(b) demonstrates the existence of TE_{11} mode waveguide behavior as the field is confined. At this point, the upper cut-off frequency side depicted in Fig. 1(c) is not suitable for the bandpass filter's simulated outcomes. The reason behind this is the location and size of the internal cavity inserted into the interior volume of the main waveguide, or the cavity's size is altered. The resonance frequency is altered by these changes, which are regarded as form perturbations [33, 34]. Thus, by integrating additional post vias to get the fine-tuning of the size of the internal cavity as shown in Fig. 2(a), the electric field distribution of this stage in Fig. 2(b) clearly shows that the field is confined in the internal cavity of the SIW structure.

Further, Fig. 2(c) shows that the reflection and transmission coefficients of the band pass filter are very selective, although a SIW filter with four perturbation vias provides better reflection and transmission coefficients. The parametric analysis was conducted to determine the optimal position of the internal vias of the SIW shown in Fig. 2(d) for achieving the desired frequency and transmission coefficient. The highlighted curve represents the final selected position of the vias. To increase the performance of a band-pass filter, a two-pole band-pass filter is more desirable than the single pole for satellite communications and X-band wireless communications. Because of its quicker roll-off and lower interference, the dual pole band-pass filter provides higher selectivity [35–37].

For cost-effective communication systems, a higher Q-factor indicates less energy loss and more efficient transmission. Two-pole band-pass filter also has a large bandwidth capacity, which is helpful for a variety of wireless applications and a high-power handling capability, which makes it appropriate for satellite and high-power wireless communications. As a result, it is favored over a bandpass filter with a single pole.

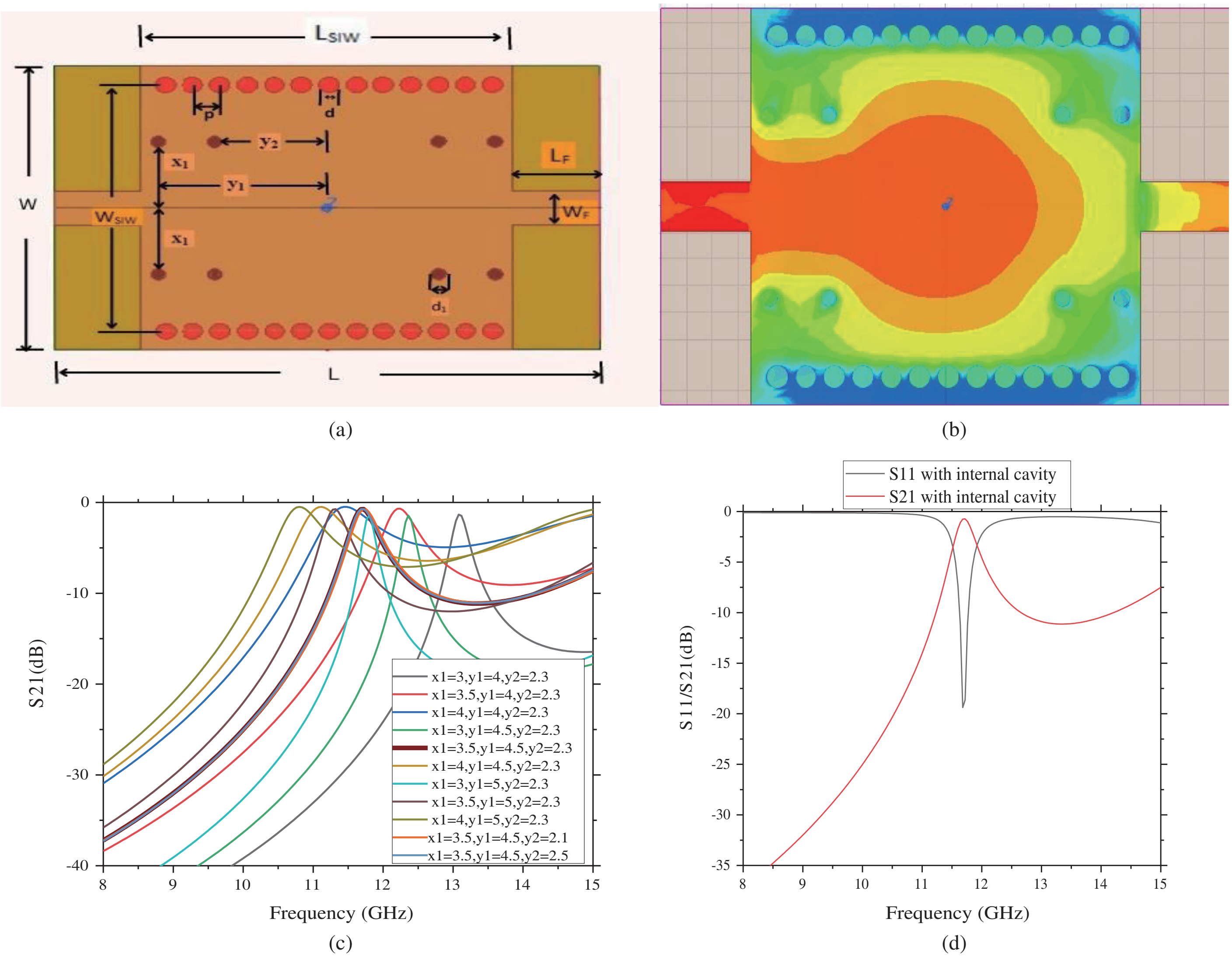

FIGURE 2. (a) Schematic of SIW bandpass filter with the internal cavity. (b) Electric field distribution of the SIW band pass filter with the internal cavity. (c) Insertion loss showing the optimal position of the internal vias. (d) Simulated results at the final position of the internal vias ($x1 = 3.5$ mm, $y1 = 4.5$ mm, $y2 = 2.3$ mm).

2.2. SIW dual Pole Band-Pass Filter Design

To convert a single-pole Substrate Integrated Waveguide (SIW) band-pass filter into a two-pole SIW band-pass filter, the single-pole SIW structure needs to be bifurcated into two resonators by inserting two more metals via post at the center of the main resonator as shown in Fig. 3(a) that divides the main resonator as resonator 1 and resonator 2. Further to make this structure tunable, the tuning element should be placed in the cavities where its TE mode's maximum electric field intensity frequently coincides with another mode's lowest in SIW rectangular resonant cavities. For TE_{102} and TE_{201} modes in particular, this is accurate. This makes it possible to install tuning elements in one mode's high-field areas without impacting the other. As a result, each mode may be adjusted separately, providing exact control and versatility when it comes to cavities [38]. To do the same thing, electric field of the SIW structure has been analyzed shown in Fig. 1(b). Electric field distribution confirms the position of via post that is suitable for tuning purposes. As shown in Fig. 3(a), metal via posts 1, 2, 3, 4 are suitable for tuning. These metallic vias end on a metallic patch at the top after short-circuiting at the lower ground plane. Fig. 3(a) shows the layout of the structure. The isolation gap that separates the metal patch from the higher ground plane creates a large capacitive load because of the developed fringing fields [39]. At the same time, resonators 1 and 2 generate two poles at a higher frequency in comparison to the whole resonator itself as shown in Fig. 3(c). The graph shows how the reflection coefficient changes with frequency at different vertical positions (x3) of center vias. It also shows the effect of varying the size of the cylindrical slot in which the capacitor is placed, as depicted in Fig. 3(c). The curve for the reflection coefficient with the final dimensions is highlighted in Fig. 3(d).

2.3. SIW Dual-Pole Band-Pass Filter with Tuning Mechanism

SIW tuning using capacitors is incorporated into the design of tunable filters, as shown in Fig. 4(a), and all physical dimen-

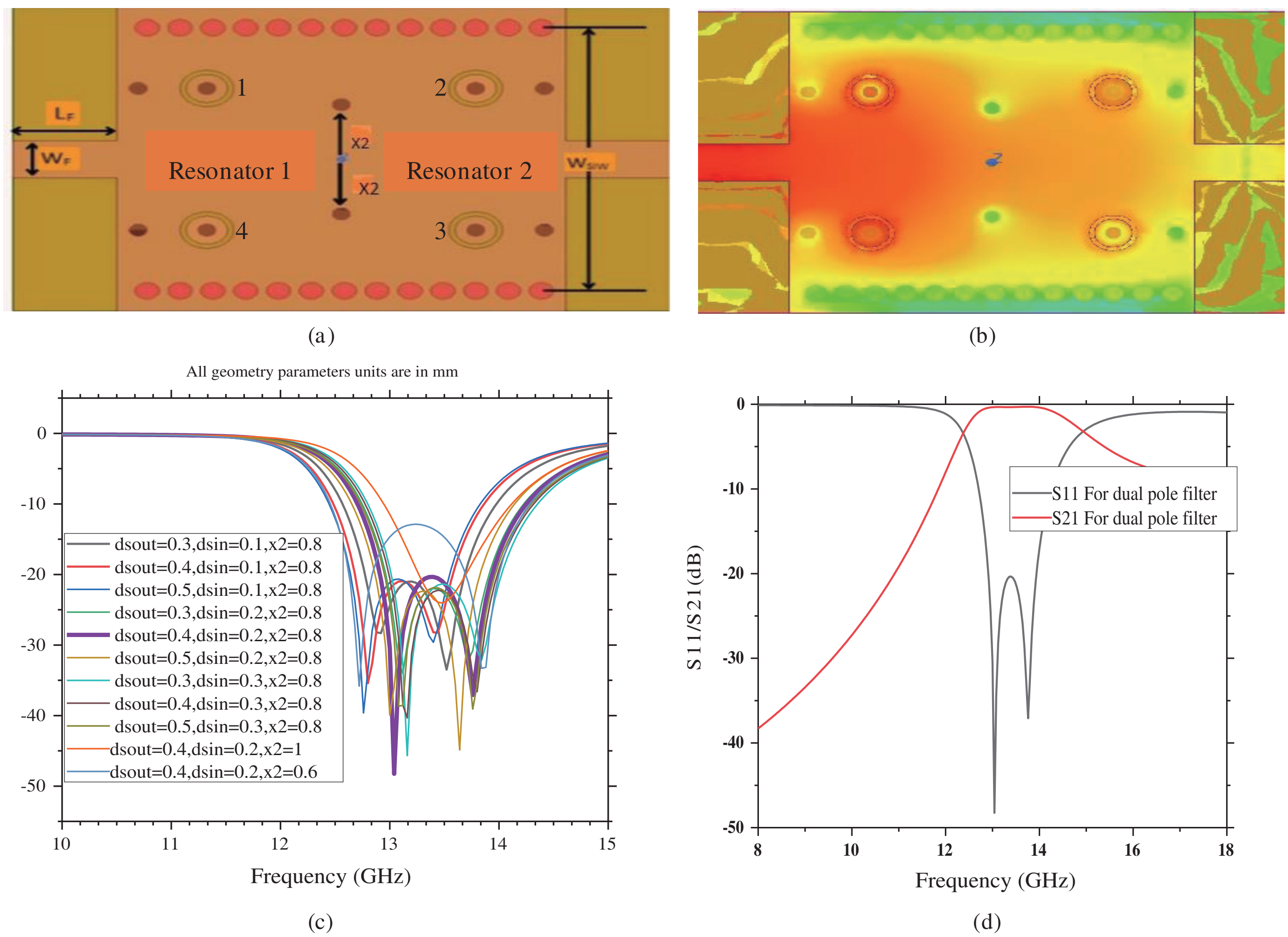

FIGURE 3. (a) Schematic of SIW dual pole band pass filter. (b) Electric Field distribution of SIW dual pole band pass filter. (c) S11 at various geometrical positions of the central vias (x2) and ring slot dimensions (dsout & dsin). (d) Simulated results for the finalized dimension (x2 = 0.8 mm, dsout = 0.4 mm, dsin = 0.2 mm).

TABLE 1. Geometrical parameters of the customizable SIW-based dual pole BPF [Unit: mm].

Symbol	Value	Symbol	Value
L	22	Y_2	2.3
L_{SIW}	13	d_1	0.6
W	15	X_1	3.5
W_{SIW}	13	Y_1	4.5
L_{F}	3.5	dsin	0.2
W_{F}	1.8	dsout	0.4
P	1.1	X_1	0.8
d	0.82		

sions of the filter are mentioned in Table 1. Resonator 1 and Resonator 2, which are identical, are positioned apart by an inductive coupling window in this setup. The coupling between the resonant modes is adjusted by the vertical position of the central metal via posts in the coupling window, whereas the resonant frequency is mostly altered by the capacitors mounted across the ring slots inside each resonator. The cavities were simulated using the Rogers 5880 with a substrate thickness of 0.51 mm. To evaluate tunable performance, central frequency tuning components are inserted and placed tactically inside the cavity. Fig. 4(a) illustrates the design of tunable filters with SIW tuning (using capacitors) for better performance. In this configuration, Resonator 1 and Resonator 2, which are identical, are spaced apart by an inductive coupling window, while

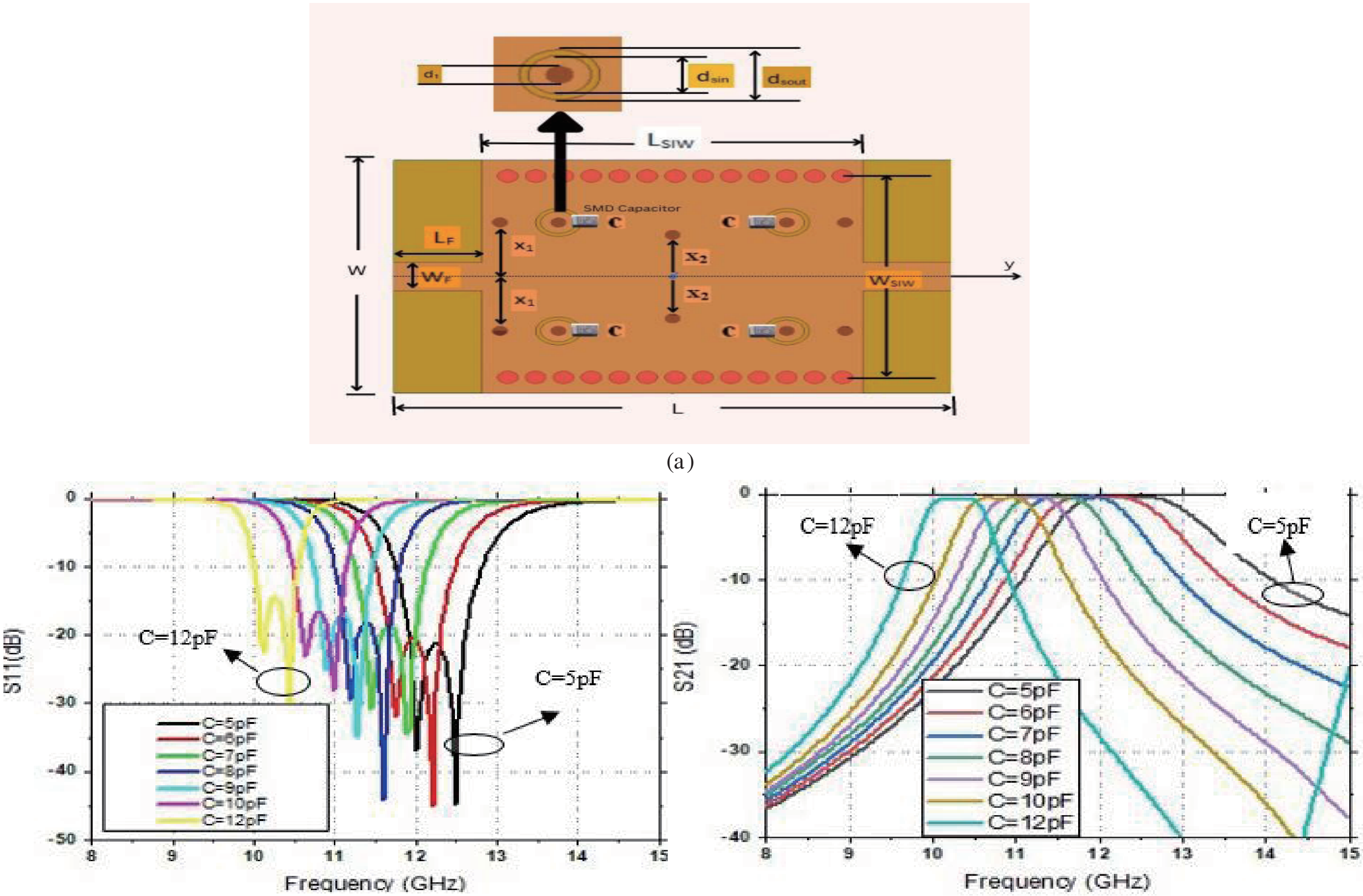

FIGURE 4. Customizable SIW-based dual pole band pass filter. (a) Final Schematic. (b) & (c) reflection & transmission coefficients at different values of the capacitor.

TABLE 2. Extracted parameters of the proposed customizable SIW-based dual pole bandpass filter.

Capacitor value (pF)	f_0 (GHz)	BW (GHz)	FBW (%)	Reflection coefficient (dB)	Transmission coefficient (dB)	Q Factor
5	12.25	1.1	8.9	> -36	-0.2	11.8
6	11.99	0.98	8.1	> -32	-0.2	12.5
7	11.7	0.92	7.8	> -31	-0.3	12.71
8	11.4	0.80	7	> -28	-0.3	14.25
9	11.1	0.76	6.8	> -26	-0.3	14.6
10	10.85	0.7	6.4	> -24	-0.4	16.87
12	10.25	0.5	4.8	> -22	-0.4	21.33

tuning elements within the resonators primarily modifies the resonant frequency and coupling between the resonant modes. Figs. 4(b) and 4(c) show the frequency tuning of the dual-pole band-pass filter for different values of the capacitor ranging from 5 pF to 12 pF. As can be seen from Table 2 by increasing the capacitor value (5 pF to 12 pF) resonance frequency shifts toward the lower side (12.25 to 10.25 GHz) of the X band range with bandwidth greater than 500 MHz. Thus, the application of capacitors as a tuning element not only provides the tuning but also reduces the overall size of the filter by choosing the higher values of the capacitor. Simulated reflection and transmission coefficients for the proposed filter are shown in Figs. 4(a) and 4(b) and summarized in Table 2 demonstrating that bandwidth & quality factors are inversely proportional because by increasing the SMT capacitor value, absolute bandwidth decreases from 1.1 GHz to 0.5 GHz, and quality factor increases from 11.8 to 21.33.

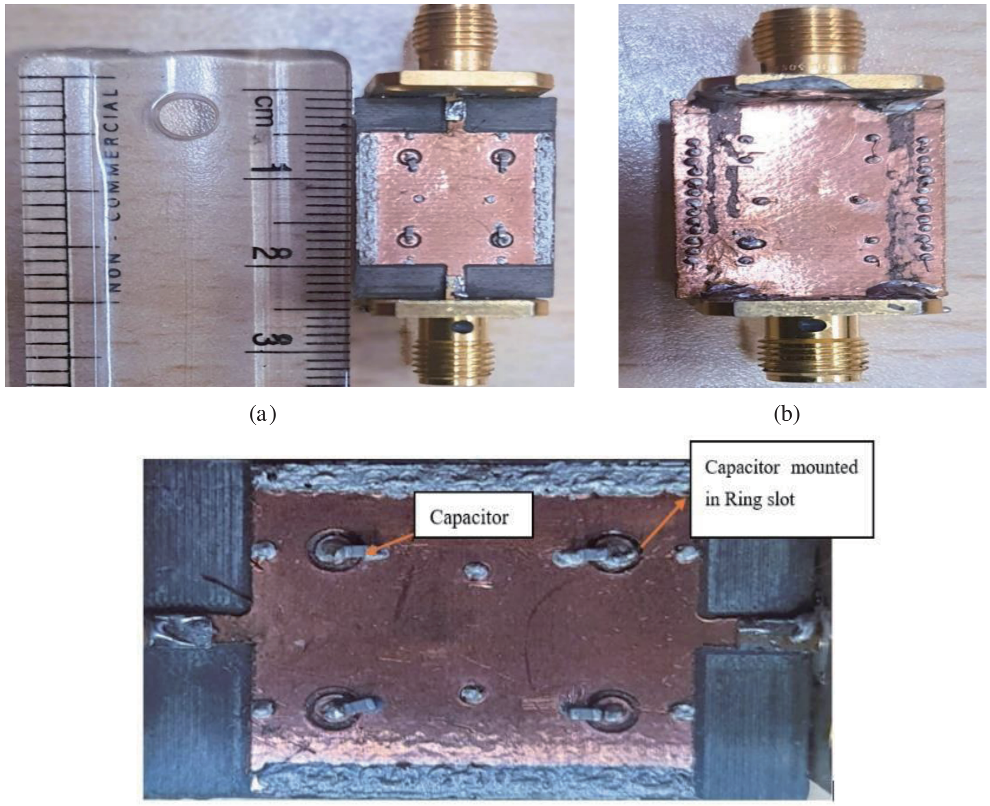

FIGURE 5. Fabricated prototype of the proposed customizable dual pole SIW band pass filter. (a) Top view. (b) Bottom view. (c) Magnified top view showing capacitor placement across ring slot.

TABLE 3. Comparison of the proposed work with earlier reported structures.

	Technique	Tuning Range (GHz)	% FBW (GHz)	Insertion loss (dB)	No of poles	Remark
[20]	Use of dielectric material rod cavities	10–11.97	18	1.5–1.8	3	Fabrication complexity (difficult to fabricate the exact diameter rod)
[21]	Mechanical Screw/flap	9.5–10.5	10	4.5	3	Difficult to adjust the flap angle
[22]	Use of capacitor	3.6–5	32	2.3–3.4	3	Complex Structure
[23]	Use of Metal Via post	4.96–5.84	22	0.2–1.1	2	Simple structure
This work	Use of Capacitor	10.25–12.25	18	0.4	2	Simple structure, (easy to integrate)

3. EXPERIMENTAL VALIDATION

To check the functionality of the simulated design in the HFSS simulation software, the prototype of the proposed customizable tuned dual-pole SIW band-pass filter is fabricated in the lab. Figs. 5(a) and 5(b) show top and bottom views of the fabricated circuit. As seen in Fig. 5(c), SMT capacitors of different values are inserted one at a time into all four ring slots of 2 mm thickness in both cavities of SIW BPF to test the tuning properly. Initially, the filter with capacitor value $C = 5$ pF is measured. One by one, the capacitor value $C = 7$ pF is inserted into the same structure & measured.

Two sets of S parameter measurements of the fabricated filter are obtained using the Agilent E8364 PNA Network analyzer. Fig. 6(a) & 6(b) show the S parameter response for $C = 5$ pF & $C = 7$ pF, respectively. In both cases, simulated results agree well with the measured ones. Minor differences between simulated and measured findings may be due to several factors, such as parasitic components from subpar soldering and capacitor leads. Variations of capacitance values in the operating band also affect the discrepancy. The simulator uses set values for the lumped RLC border, unlike the real capacitor that exhibits increasing capacitance with frequency. Additionally, the capacitive impact of the ring slot was not taken into account, caus-

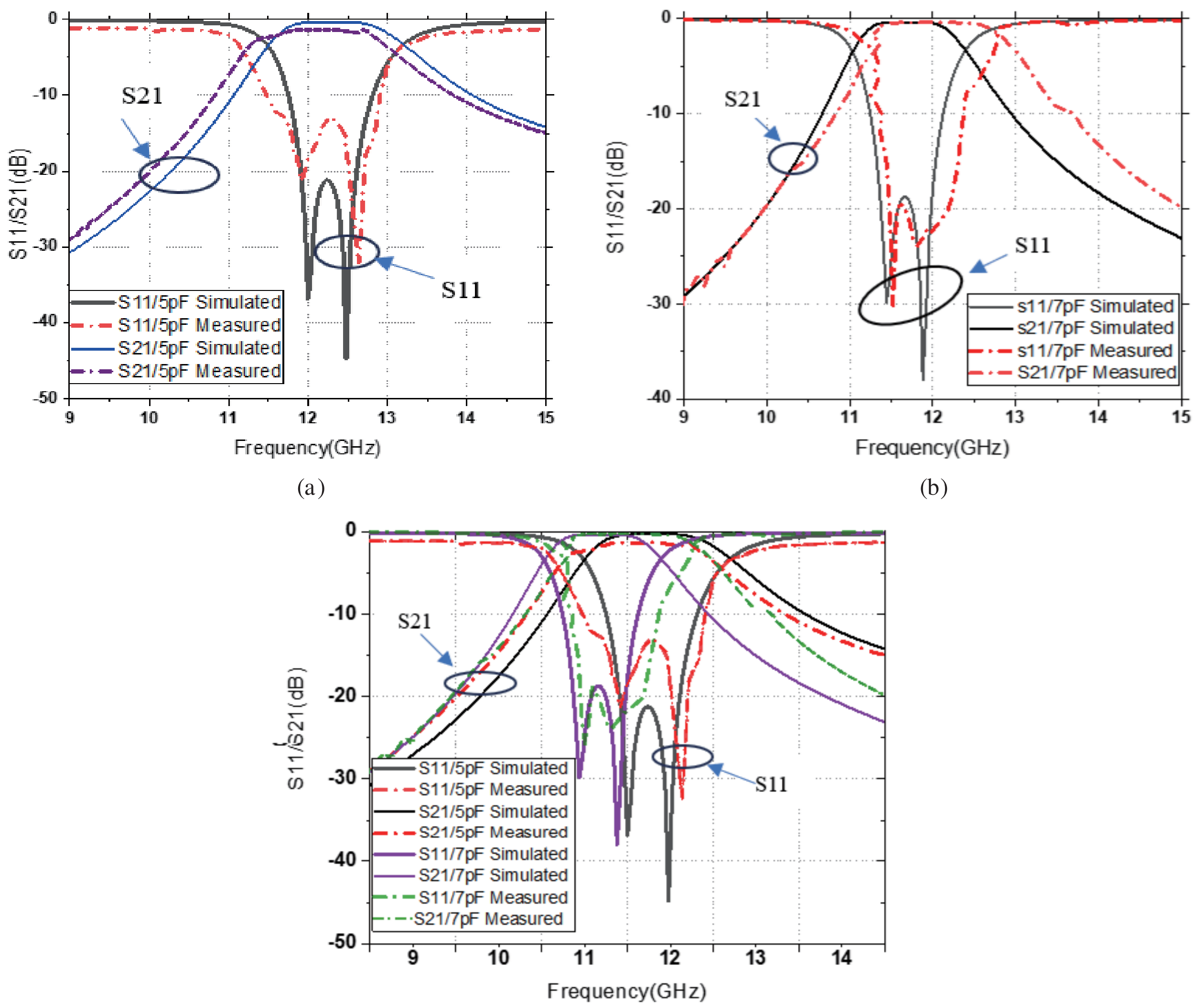

FIGURE 6. Simulated and measured results of the fabricated filter with two different values of the capacitor, (a) S-parameters at $C = 5$ pF, (b) S-Parameters at $C = 7$ pF, (c) S-parameters showing the combined results for $C = 5$ pF & 7 pF.

ing a lack of accuracy in the measured response. The measured and simulated filter responses for these two cases are displayed in Figs. 6(a) & (b). In this instance, the filter's passband has been moved from 12.25 to 11.75 GHz, and a total tunability of 500 MHz has been accomplished.

Therefore, the center frequency with a tunability of up to 4.2% is reported with this straightforward tuning that involves placing different capacitor values (5 pF & 7 pF) across the ring slot surrounding the perturbation via post. Even though the experimental results are restricted to the usage of discrete capacitors alone, they nonetheless serve as proof of concept (PoC) for the design. Due to fabrication constraints, only two capacitor values can be measured for validation purposes. However, simulation results show a wide range of tunability up to 17.7% with different values of capacitors ranging from 5 pF to 12 pF. The tunability of the filter can be observed from the simulated results shown in Fig. 6(c) by changing the capacitor value mounted on the cavity vias. The transmission coefficient better than 0.4 dB is obtained in the specified frequency range with a fractional bandwidth (FBW) greater than 4% and a quality factor better than 11.8 which is considered to be optimum for the Bandpass filter.

The performance of the proposed filter is compared in Table 3, with previously reported tuning (customizable) methods compared. After comparison, it can be observed that the proposed filter is simple in geometry and has better insertion loss. It can be easily implemented and scalable to a required frequency.

4. CONCLUSION

A customizable SIW-based band-pass filter to be used for X-band frequencies has been introduced. It has been observed that by simply altering the SMT capacitor value from 5 pF to 12 pF, the center frequency of the filter can be varied. In contrast to conventional BP-BS cascaded filters, this newly proposed filter offers the distinct advantage of simplicity in geometry and better insertion loss. It is envisaged that the proposed filter can be made using conventional PCB materials and fabrication techniques, and it holds significant potential for easier integration with planar circuitry. The practicality of this design has been confirmed through testing and fabrication, with experimental results closely aligning with the results obtained from simulations. Furthermore, with the recent increasing interest in high-frequency applications, investigations of the proposed design can be done at high frequency as well.

REFERENCES

[1] Kanth, V. K. and S. Raghavan, "EM design and analysis of a substrate integrated waveguide based on a frequency-selective surface for millimeter wave radar application," *Journal of Computational Electronics*, Vol. 18, No. 1, 189–196, Mar. 2019.

[2] Rehman, M. Z. U., Z. Baharudin, M. A. Zakariya, M. H. M. Khir, M. T. Khan, and P. W. Weng, "Recent advances in miniaturization of substrate integrated waveguide bandpass filters and its applications in tunable filters," in *2013 IEEE Business Engineering and Industrial Applications Colloquium (BEIAC)*, 109–114, IEEE, Langkawi, Malaysia, Apr. 2013.

[3] Iqbal, A., J. J. Tiang, S. K. Wong, M. Alibakhshikenari, F. Falcone, and E. Limiti, "Miniaturization trends in substrate integrated waveguide (SIW) filters: A review," *IEEE Access*, Vol. 8, 223 287–223 305, 2020.

[4] Jones, T. R. and M. Daneshmand, "Miniaturized folded ridged half-mode and quarter-mode substrate integrated waveguides for filter design," *IEEE Transactions on Microwave Theory and Techniques*, Vol. 67, No. 8, 3414–3426, Aug. 2019.

[5] Grigoropoulos, N., B. Sanz-Izquierdo, and P. R. Young, "Substrate integrated folded waveguides (SIFW) and filters," *IEEE Microwave and Wireless Components Letters*, Vol. 15, No. 12, 829–831, Dec. 2005.

[6] Kumar, S. and A. De, "Cavity-backed slot loaded substrate integrated waveguide self-diplexing antenna for C band applications," in *2022 IEEE 6th Conference on Information and Communication Technology (CICT)*, 1–4, IEEE, 2022.

[7] Pelluri, S., M. Fasil, and M. V. Kartikeyan, "Miniaturized wide stopband half-mode SIW bandpass filter," in *2019 IEEE MTT-S International Microwave and RF Conference (IMARC)*, IEEE, Mumbai, India, Dec. 2019.

[8] Azad, A. R. and A. Mohan, "Substrate integrated waveguide dual-band and wide-stopband bandpass filters," *IEEE Microwave and Wireless Components Letters*, Vol. 28, No. 8, 660–662, Aug. 2018.

[9] Shen, Y.-L., J.-T. Hung, M.-H. Ho, and C.-I. G. Hsu, "Miniaturised substrate integrated waveguide cavities in dual-band filter and diplexer design," *IET Microwaves, Antennas & Propagation*, Vol. 14, No. 5, 428–434, Apr. 2020.

[10] Kumar, A. and S. Srivastava, "SIW cavity-backed dual inverted L slot antenna array for Ku band applications," *International Journal of Microwave and Wireless Technologies*, Vol. 15, No. 1, 150–155, 2023.

[11] Tewari, N., N. Joshi, and S. Srivastava, "A miniaturized aperture-coupled 4×4 MIMO array SIW antenna at K band," *Microwave and Optical Technology Letters*, Vol. 66, No. 1, e33952, Jan. 2024.

[12] Muchhal, N., A. Chakraborty, T. Agrawal, and S. Srivastava, "Miniaturized and selective half-mode substrate integrated waveguide bandpass filter using Hilbert Fractal for sub-6 GHz 5G applications," *IETE Journal of Research*, Vol. 69, 6685–6692, 2022.

[13] Entesari, K., A. P. Saghati, V. Sekar, and M. Armendariz, "Tunable SIW structures: antennas, VCOs, and filters," *IEEE Microwave Magazine*, Vol. 16, No. 5, 34–54, 2015.

[14] Memon, M. U. and S. Lim, "Review of reconfigurable substrate-integrated-waveguide antennas," *Journal of Electromagnetic Waves and Applications*, Vol. 28, No. 15, 1815–1833, Oct. 2014.

[15] Yang, S., C. Zhang, H. K. Pan, A. E. Fathy, and V. K. Nair, "Frequency-reconfigurable antennas for multiradio wireless platforms," *IEEE Microwave Magazine*, Vol. 10, No. 1, 66–83, Feb. 2009.

[16] Rebeiz, G. M., K. Entesari, I. C. Reines, S.-J. Park, M. A. El-Tanani, A. Grichener, and A. R. Brown, "Tuning in to RF MEMS," *IEEE Microwave Magazine*, Vol. 10, No. 6, 55–72, Oct. 2009.

[17] Abdollahvand, M., E. Martinez-de Rioja, K. Forooraghi, Z. Atlasbaf, J. A. Encinar, S. Ghosh, and A. Ebrahimi, "Active frequency selective surface with switchable response for satellite communications in X and Ka bands," *International Journal of RF and Microwave Computer-Aided Engineering*, Vol. 32, No. 9, e23255, Sep. 2022.

[18] Al-Yasir, Y. I., N. O. Parchin, R. A. Abd-Alhameed, A. M. Abdulkhaleq, and J. M. Noras, *A Survey of Microwave Reconfigurable Filters for 5G Systems: Recent Advances and Future Challenges*, 96, Microwave/RF Components for 5G Front-End Systems, 2019.

[19] Meyer, E., "Tunable narrow-band X-band bandpass filters," Ph.D. dissertation, Stellenbosch: Stellenbosch University, 2018.

[20] De, S., S. K. Koul, and K. K. Samanta, "Low profile dielectric rod tuned reconfigurable band pass filters," *IEEE Journal of Microwaves*, Vol. 2, No. 3, 507–521, Jul. 2022.

[21] Mira, F., J. Mateu, and C. Collado, "Mechanical tuning of substrate integrated waveguide filters," *IEEE Transactions on Microwave Theory and Techniques*, Vol. 63, No. 12, 3939–3946, Dec. 2015.

[22] Hung, S.-Y., G.-P. Li, and Y. Guo, "Compact customisable bandstop-bandpass-bandstop cascaded filter based on substrate integrated waveguide coax cavities," *IET Microwaves, Antennas & Propagation*, Vol. 14, No. 4, 281–292, Mar. 2020.

[23] Caleffo, R. C. and F. S. Correra, "Determining a perturbation factor to design tunable resonant cavities in SIW technology," *Journal of Microwaves, Optoelectronics and Electromagnetic Applications*, Vol. 22, 230–242, 2023.

[24] Li, J., J. Chen, P. Chen, and F. Zhu, "Varactor-tuned half mode substrate integrated waveguide reflection-type phase shifter," in *2012 IEEE MTT-S International Microwave Workshop Series on Millimeter Wave Wireless Technology and Applications*, 1–3, Nanjing, China, 2012.

[25] Pantoli, L., V. Stornelli, and G. Leuzzi, "A single-transistor tunable filter for bluetooth applications," in *2012 42nd European Microwave Conference*, 889–892, Amsterdam, Netherlands, 2012.

[26] Lugo, C. and J. Papapolymerou, "Electronic switchable bandpass filter using PIN diodes for wireless low cost system-on-a-package applications," *IEE Proceedings — Microwaves, Antennas and Propagation*, Vol. 151, No. 6, 497–502, 2004.

[27] Entesari, K., A. P. Saghati, V. Sekar, and M. Armendariz, "Tunable SIW structures: antennas, VCOs, and filters," *IEEE Microwave Magazine*, Vol. 16, No. 5, 34–54, 2015.

[28] Rebeiz, G. M., K. Entesari, I. C. Reines, S.-J. Park, M. A. El-Tanani, A. Grichener, and A. R. Brown, "Tuning in to RF MEMS," *IEEE Microwave Magazine*, Vol. 10, No. 6, 55–72, Oct. 2009.

[29] Jones, T. R. and M. Daneshmand, "Miniaturized folded ridged quarter-mode substrate integrated waveguide RF MEMS tunable bandpass filter," *IEEE Access*, Vol. 8, 115 837–115 847, 2020.

[30] De, S., S. K. Koul, and K. K. Samanta, "Miniaturized reconfigurable band pass filters," in *2021 IEEE MTT-S International Microwave and RF Conference (IMARC)*, 1–4, IEEE, Dec. 2021.

[31] Deslandes, D. and K. Wu, "Integrated microstrip and rectangular waveguide in planar form," *IEEE Microwave and Wireless Components Letters*, Vol. 11, No. 2, 68–70, Feb. 2001.

[32] Wu, K., D. Deslandes, and Y. Cassivi, "The substrate integrated circuits — A new concept for high-frequency electronics and optoelectronics," in *6th International Conference on Telecommunications in Modern Satellite, Cable and Broadcasting Service, 2003. TELSIKS 2003.*, P3–P10, Nis, Yugoslavia, Oct. 2003.

[33] Ramo, S., J. R. Whinnery, and T. V. Duzer, *Fields and Waves in Communication Electronics*, 3rd ed., John Wiley & Sons, 1994.

[34] Ali, J. K. and N. N. Hussain, "An extra reduced size dual-mode bandpass filter for wireless communication systems," in *PIERS Preceedings*, 1467–1470, Suzhou, China, Sep. 2011.

[35] Pradhan, N. C., S. Koziel, R. K. Barik, A. Pietrenko-Dabrowska, and S. S. Karthikeyan, "Miniaturized dual-band SIW-based bandpass filters using open-loop ring resonators," *Electronics*, Vol. 12, No. 18, 3974, Sep. 2023.

[36] Abdollahvand, M., G. Dadashzadeh, and D. Mostafa, "Compact dual band-notched printed monopole antenna for UWB application," *IEEE Antennas and Wireless Propagation Letters*, Vol. 9, 1148–1151, 2010.

[37] Cho, Y.-H. and G. M. Rebeiz, "Two-and four-pole tunable 0.7–1.1-GHz bandpass-to-bandstop filters with bandwidth control," *IEEE Transactions on Microwave Theory and Techniques*, Vol. 62, No. 3, 457–463, 2014.

[38] Rezaee, M. and A. R. Attari, "Analytical calculation of the resonant frequencies for a corner cut square SIW cavity," in *2016 24th Iranian Conference on Electrical Engineering (ICEE)*, 517–520, Shiraz, Iran, May 2016.

[39] Wang, J., R. Wang, L. Li, J. Guo, and J. Zhang, "Design of a new capacitive load cross-coupled cavity filter," *Electronics*, Vol. 12, No. 1, 142, 2023.